Improved Detection of Transosseous Meningiomas Using ^{68}Ga-DOTATATE PET/CT Compared with Contrast-Enhanced MRI

Wolfgang G. Kunz[1], Lisa M. Jungblut[1], Philipp M. Kazmierczak[1], Franziska J. Vettermann[2], Andreas Bollenbacher[2], Jörg C. Tonn[3], Christian Schichor[3], Axel Rominger[2], Nathalie L. Albert[2], Peter Bartenstein[2], Maximilian F. Reiser[1], and Clemens C. Cyran[1]

[1]Institute for Clinical Radiology, Ludwig-Maximilians-University Hospital, Munich, Germany; [2]Department of Nuclear Medicine, Ludwig-Maximilians-University Hospital, Munich, Germany; and [3]Department of Neurosurgery, Ludwig-Maximilians-University Hospital, Munich, Germany

^{68}Ga-DOTATATE PET/CT enables detection of meningioma tissue based on somatostatin receptor 2 expression. Transosseous extension of intracranial meningiomas is known to be an important risk factor for tumor recurrence and patient mortality. We analyzed the diagnostic performance of ^{68}Ga-DOTATATE PET/CT and contrast-enhanced MRI (CE-MRI) for the detection of osseous infiltration using qualitative and quantitative imaging parameters. **Methods:** In this institutional review board–approved retrospective study, subjects were selected from 327 consecutive ^{68}Ga-DOTATATE PET/CT examinations for evaluation of confirmed or suspected meningioma. Inclusion criteria were CE-MRI within 30 d and pathology-confirmed meningioma diagnosis with inclusion or exclusion of transosseous extension as the standard of reference. Imaging was analyzed by two readers. Tracer uptake values and meningioma volumes were determined. χ^2, Mann–Whitney U, Wilcoxon signed rank, and McNemar tests, as well as receiver-operating-characteristic analyses, were performed to compare variables and diagnostic performance. **Results:** Eighty-two patients fulfilled the inclusion criteria. Patients with transosseous extension of meningioma ($n = 67$) showed significantly larger lesions (median, 12.8 vs. 3.3 mL; $P < 0.001$) and significantly higher tracer uptake values (median SUV_{max}, 14.2 vs. 7.6; $P = 0.011$) than patients with extraosseous meningiomas ($n = 15$). ^{68}Ga-DOTATATE PET/CT in comparison to CE-MRI performed at a higher sensitivity (98.5% vs. 53.7%) while maintaining high specificity (86.7% vs. 93.3%) in the detection of osseous involvement ($P < 0.001$). In receiver-operating-characteristic analysis, PET/CT assessment performed better than CE-MRI (area under the curve, 0.932 vs. 0.773). PET/CT- and CE-MRI–based volume estimation yielded comparable results for extraosseous meningiomas ($P = 0.132$) and the extraosseous part of transosseous meningiomas ($P = 0.636$), whereas the volume of the intraosseous part was assessed as significantly larger by PET/CT ($P < 0.001$). **Conclusion:** ^{68}Ga-DOTATATE PET/CT enables improved detection of the transosseous extension of intracranial meningiomas compared with CE-MRI.

Key Words: meningioma; osseous involvement; PET-CT; ^{68}Ga-DOTATATE; MRI

J Nucl Med 2017; 58:1580–1587
DOI: 10.2967/jnumed.117.191932

Meningiomas are the most common intracranial neoplasms, representing approximately one third of all newly diagnosed primary central nervous system tumors in recent years (*1*). The recently published European Association of Neuro-Oncology guidelines for the diagnosis and treatment of meningiomas by Goldbrunner et al. recommend MRI as the primary radiologic modality of choice (*2*). The MRI diagnosis of meningioma relies on a morphologic analysis, which can be supplemented by CT. In recent decades, new molecular imaging strategies based on PET have evolved and allow the incorporation of functional information for diagnostic purposes (e.g., glucose metabolism using ^{18}F-FDG (*3,4*) or somatostatin receptor 2 expression using ^{68}Ga-DOTATATE (*5–7*)). In particular, ^{68}Ga-DOTATATE PET/CT imaging has demonstrated benefits for noninvasive differential diagnosis (*8*), treatment planning (*9–11*), and growth prediction (*12*).

Transosseous extension of intracranial meningiomas has been identified as an important risk factor for tumor recurrence and patient mortality (*13–16*), as it frequently impedes gross total resection. The detection of osseous infiltration has relied on morphologic features such as hyperostosis or intraosseous contrast enhancement, which, however, provide only limited diagnostic value (*17–20*). A new approach for improved detection of osseous involvement was established for PET/CT imaging with the tracer ^{18}F-fluoride (*21,22*), which indirectly demonstrates meningioma-induced bone changes. However, a systematic analysis for the detection of osseous involvement by the tracer ^{68}Ga-DOTATATE, which depicts the meningioma-characteristic somatostatin receptor 2 expression, is still lacking.

The aim of our study was to evaluate the diagnostic performance of ^{68}Ga-DOTATATE PET/CT imaging and contrast-enhanced MRI (CE-MRI) for the qualitative detection of osseous involvement in pre- and postoperative clinical time points using pathology-proven osseous infiltration as the standard of reference. In addition, we investigated quantitative ^{68}Ga-DOTATATE PET/CT and CE-MRI parameters; tumor-to-background signals;

Received Feb. 17, 2017; revision accepted Apr. 11, 2017.
For correspondence or reprints contact: Wolfgang G. Kunz, Institute for Clinical Radiology, Ludwig-Maximilians-University Hospital Munich, Marchioninistraße 15, 81377 Munich, Germany.
E-mail: wolfgang.kunz@med.lmu.de
Published online Apr. 27, 2017.

TABLE 1
Characteristics of Extraosseous and Transosseous Meningiomas

Parameter	Variable	Extraosseous (n = 15)	Transosseous (n = 67)	P
Age (y)		55 (51–66)	49 (47–61)	0.073
Male sex		6 (40%)	13 (19%)	0.087
Pathology				
WHO grade	I	9 (60%)	56 (84%)	NA
	II	6 (40%)	9 (13%)	
	III	0 (0%)	2 (3%)	
Histologic subtype	Transitional	5 (38%)	22 (38%)	NA
	Meningothelial	2 (15%)	15 (26%)	
	Microcystic	0 (0%)	4 (7%)	
	Fibroblastic	0 (0%)	1 (2%)	
	Secretory	0 (0%)	5 (9%)	
	Atypical	6 (46%)	9 (16%)	
	Anaplastic	0 (0%)	2 (3%)	
Qualitative imaging				
Meningiomatosis		9 (60%)	26 (39%)	0.134
Location	Parasagittal/parafalcine	5 (33%)	10 (15%)	NA
	Convexity	6 (40%)	12 (18%)	
	Sphenoid wing	3 (20%)	42 (63%)	
	Cerebellopontine	0 (0%)	2 (3%)	
	Suprasellar/parasellar	1 (7%)	1 (1%)	
PET/CT for osseous involvement	No signs of	13 (87%)	0 (0%)	NA
	Suggestive of	0 (0%)	1 (1%)	
	Consistent with	2 (13%)	66 (99%)	
CE-MRI for osseous involvement	No signs of	9 (60%)	12 (18%)	NA
	Suggestive of	5 (33%)	19 (28%)	
	Consistent with	1 (7%)	36 (54%)	
Peritumoral edema	None	8 (53%)	33 (49%)	0.858
	Mild	3 (20%)	18 (27%)	
	Extensive	4 (27%)	16 (24%)	
Quantitative imaging				
Meningioma volume in PET/CT (mL)		3.3 (1.6–4.7)	12.8 (6.8–32.9)	<0.001*
Meningioma volume in CE-MRI (mL)		2.5 (1.4–4.7)	10.6 (4.6–22.0)	0.001*
Meningioma SUV_{max}		7.6 (4.3–13.9)	14.2 (10.0–22.4)	0.011*
Meningioma SUV_{mean}		2.7 (1.9–3.0)	4.3 (3.1–5.9)	0.001*
Pituitary SUV_{max}		15.8 (12.9–20.0)	15.7 (11.6–19.3)	0.852
Pituitary SUV_{mean}		3.7 (3.5–4.2)	4.0 (3.3–4.7)	0.587

*Statistically significant.
WHO = World Health Organization; NA = not applicable.
Data are count followed by percentage for categoric variables and median followed by interquartile range for continuous variables. Proportion analysis was tested using χ^2 test. Nonparametric testing for continuous variables was performed using Mann–Whitney U test.

and volume estimation of total, intraosseous, and extraosseous parts using both methods.

MATERIALS AND METHODS

Study Design and Population

The institutional review board of the Ludwig-Maximilians-University Hospital, Munich (Ethikkommission der Medizinischen Fakultät der Ludwig-Maximilians-Universität München), approved this retrospective study and waived the requirement for informed consent. This study was conducted according to the Helsinki Declaration of 1975 (and as revised in 2013). The study was based on a consecutive cohort of 327 patients evaluated with ^{68}Ga-DOTATATE PET/CT for confirmed or suspected intracranial meningioma at our institution between August 2010 and January 2016.

Of this cohort, we included all subjects with CE-MRI within 30 d of either pre- or postoperative matching ^{68}Ga-DOTATATE PET/CT imaging and a pathology-confirmed meningioma diagnosis with inclusion or exclusion of transosseous extension. We excluded all subjects who had a diagnosis other than meningioma, who had undergone repeated examinations, or whose PET/CT or MR images were not of diagnostic quality.

PET/CT and MR Image Acquisition

All patients underwent ^{68}Ga-DOTATATE PET/CT (Biograph 64; Siemens Healthcare) 60 min after intravenous injection of a median 150 MBq (interquartile range, 129–187 MBq) of ^{68}Ga-DOTATATE. First, contrast-enhanced CT scans (1.5 mL of iopromide [Ultravist-300; Bayer Healthcare] per kilogram of body weight) were obtained for anatomic localization. Subsequently, the PET scan was acquired by static emission data for 4 min per bed position. PET images were reconstructed using an iterative algorithm (ordered-subset expectation maximization: 4 iterations, 8 subsets). Contrast-enhanced CT data were reconstructed with a slice thickness of 2.0 mm (axial). The reconstructed PET, CT, and fused images were analyzed on the manufacturer's imaging software (syngo.via; Siemens Healthcare). MRI was performed on 1.5- or 3.0-T scanners across different manufacturers. The protocol consisted of axial T2-weighted sequences (slice thickness of 2.0 mm), fluid-attenuated inversion recovery sequences (slice thickness of 5.0 mm), diffusion-weighted imaging (slice thickness of 5.0 mm), and 3-dimensional T1-weighted sequences (slice thickness of 1.0 mm) before and after administration of an intravenous contrast agent, gadobutrol (Gadovist; Bayer Healthcare) (0.1 mL of a 1.0 mmol/mL solution per kilogram of body weight).

Pathologic Analysis

All tumors were fixed in 4% neutral formalin for 24 h at room temperature, embedded in paraffin, and cut into consecutive 4-mm-thick sections. Pathologic diagnosis of meningioma was performed according to the current World Health Organization classification of tumors of the central nervous system (*23*). Only patients with clearly defined inclusion or exclusion of osseous involvement were considered.

Qualitative Imaging Analysis

PET/CT and corresponding CE-MRI studies were analyzed in consensus by two readers with several years of experience in hybrid imaging (one board-certified in nuclear medicine with 6 y of experience in PET/CT and MRI; the other board-certified in radiology and diagnostic nuclear medicine with 10 y of experience in PET/CT and MRI). The information from the CT, PET, and all MRI sequences was considered in establishing the diagnosis of osseous involvement. The readers were unaware of any clinical or pathologic information. Osseous involvement was assessed on a 3-point ordinal scale: 0 = no signs of; 1 = suggestive of; 2 = consistent with. Peritumoral edema was assessed on a 3-point ordinal scale: 0 = none; 1 = mild; 2 = extensive. Location and presence of meningiomatosis was noted.

Quantitative Imaging Analysis

Volumetric analyses of the total meningioma and the intraosseous part (when applicable) were performed in a masked and randomized fashion using OsiriX imaging software (version 4.0; Pixmeo). In PET/CT scans, the total volume of interest (VOI) was first determined by the tracer uptake using the software's growing-region tool with an SUV_{max} cutoff of 2.3 as determined by a previous study (*24*). Subsequently, the total VOI was manually adjusted on each slice to fit the intraosseous tracer uptake using CT overlay representations to define the intraosseous versus extraosseous parts of the meningioma. SUV_{max} and SUV_{mean} were determined for both VOIs (total and intraosseous) and the pituitary gland. In MRI scans, the total volume was determined by manually setting regions of interest on each axial slice using the software's closed-polygon tool followed by calculation of the total VOI. Subsequently, the total VOI was adjusted to fit the intraosseous tracer uptake, resulting in calculation of the intraosseous VOI. The extraosseous VOI was calculated as [total VOI − intraosseous VOI]. Measurement of the tumor-to-background signal was based on SUV_{mean} in PET/CT and signal in T1-weighted CE-MRI sequences. The contralateral nonaffected bone served as background for intraosseous parts; the contralateral subarachnoid space served as background for extraosseous parts of the meningioma.

Statistical Analysis

We performed all statistical analyses using SPSS Statistics 23 (IBM). Diagnostic accuracy was determined using 2×2 tables and is presented as sensitivity, specificity, and positive and negative likelihood ratios. As the prevalence of transosseous meningiomas in the study population does not reflect the real prevalence, we did not calculate the positive or negative predictive value, because these measures depend on the prevalence. The statistical difference between two diagnostic methods was evaluated using the McNemar test. Categoric variables were compared using the χ^2 test. Nonparametric tests for nonnormally distributed continuous variables were performed using the Mann–Whitney *U* test for independent samples and the Wilcoxon signed rank test for related samples. Correlation between nonnormally distributed continuous variables was calculated using Spearman analysis. Receiver-operating-characteristic analyses were performed to compare the diagnostic performance using area under the curve. Binary logistic regression analysis was performed to test the association between predictors and the dependent variable pathology-confirmed transosseous extension of meningioma. All continuous and nonnormally distributed variables are presented as median followed by interquartile range. Normal distribution was assessed using the Kolmogorov–Smirnov test. Categoric

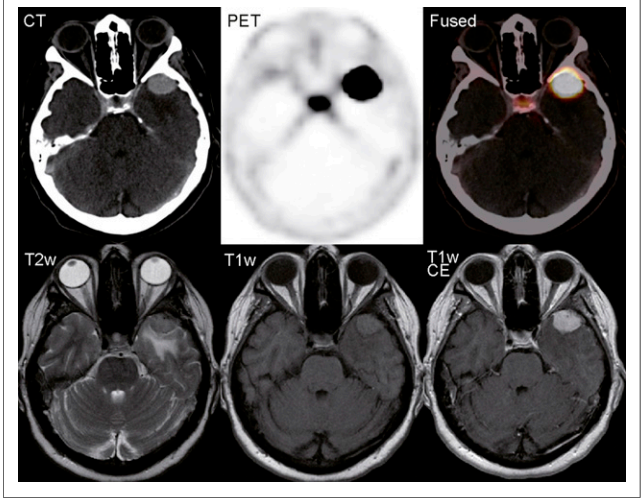

FIGURE 1. Example of meningioma with transosseous extension. A 56-y-old woman presented with worsening headache. CE-MRI was performed and revealed large, homogeneously enhancing mass in left temporopolar region, consistent with meningioma (lower row). Before surgical resection, patient was examined using ^{68}Ga-DOTATATE PET/CT, which additionally demonstrated transosseous extension as assessed by strong tracer uptake extending into sphenoid wing. This was not evident on nonenhanced T2- or T1-weighted images or on T1-weighted CE-MR images. Extension of meningioma into sphenoid wing was found during surgical resection and later confirmed by pathologic evaluation of transosseous secretory meningioma (World Health Organization grade I). w = weighted.

TABLE 2
Diagnostic Performance of ^{68}Ga-DOTATATE PET/CT and CE-MRI for Detection of Osseous Involvement in Intracranial Meningiomas

Method	Sensitivity	Specificity	Positive LR	Negative LR	Prevalence
Overall (n = 82)					
PET/CT	98.5 (92.0–99.9)	86.7 (60.0–98.3)	7.39 (2.03–26.9)	0.02 (0.00–0.12)	81.7 (71.6–89.4)
CE-MRI	53.7 (41.1–66.0)	93.3 (68.1–99.8)	8.06 (1.20–54.2)	0.50 (0.37–0.66)	81.7 (71.6–89.4)
Preoperative (n = 39)					
PET/CT	100 (88.4–100)	77.8 (40.0–97.2)	4.50 (1.33–15.3)	0.00 (NA)	76.9 (60.7–88.9)
CE-MRI	53.3 (34.3–71.7)	100 (66.4–100)	∞ (NA)	0.47 (0.32–0.68)	76.9 (60.7–88.9)
Postoperative (n = 43)					
PET/CT	97.3 (85.8–99.9)	100 (54.1–100)	∞ (NA)	0.03 (0.00–0.19)	86.0 (72.1–94.7)
CE-MRI	54.1 (36.9–70.5)	83.3 (35.9–99.6)	3.24 (0.53–19.9)	0.55 (0.33–0.91)	86.0 (72.1–94.7)

LR = likelihood ratio; NA = not applicable.
Data are percentages (or ratios) followed by 95% confidence interval. Imaging diagnosis of "consistent with" was set as test-positive. McNemar test showed significant differences in diagnostic performance of PET/CT and CE-MRI ($P < 0.001$).

variables are presented as frequency and percentage. P values below 0.05 were considered to indicate statistical significance.

RESULTS

Study Population

Among the initial cohort of 327 ^{68}Ga-DOTATATE PET/CT examinations, 42 patients had diagnoses other than meningioma. Of the remaining 285 examinations, 82 were repeated examinations of the same patient. Of 203 individual patients with an imaging-based diagnosis of meningioma, 86 did not have a corresponding MRI examination within 30 d of PET/CT and 12 had nondiagnostic MRI examinations. The remaining 105 patients were analyzed for morphologic and functional parameters. The final study cohort for the diagnostic accuracy analysis was formed by 82 patients for whom additional pathologic evaluation of osseous involvement was available. A detailed flow chart of patient selection is presented in Supplemental Figure 1 (supplemental materials are available at http://jnm.snmjournals.org).

TABLE 3
Receiver-Operating-Characteristic Analysis of Imaging Parameters for Osseous Involvement

Parameter	Area under curve	P
PET/CT qualitative assessment	0.932 (0.830–1.000)	<0.001*
PET/CT meningioma volume	0.803 (0.681–0.925)	<0.001*
PET/CT meningioma SUV_{mean}	0.778 (0.640–0.916)	0.001*
CE-MRI qualitative assessment	0.773 (0.637–0.909)	0.001*
CE-MRI meningioma volume	0.768 (0.641–0.895)	0.001*
PET/CT meningioma SUV_{max}	0.710 (0.557–0.864)	0.011*
PET/CT peritumoral edema	0.508 (0.342–0.675)	0.919
CE-MRI peritumoral edema	0.477 (0.307–0.646)	0.778

*Statistically significant.
95% confidence intervals are in parentheses.

Characteristics of Extraosseous and Transosseous Meningiomas

In the final study population for diagnostic accuracy evaluation, 15 patients (18.3%) had extraosseous meningiomas and 67 patients (81.7%) transosseous meningiomas. The transosseous meningioma patients had a significantly higher meningioma SUV_{max} (14.2 vs. 7.6; $P = 0.011$) and SUV_{mean} (4.3 vs. 2.7; $P = 0.001$) than the extraosseous meningioma patients, whereas the pituitary gland values did not significantly differ (each with $P > 0.05$). Transosseous meningiomas had significantly larger volumes, whether assessed by PET/CT (12.8 vs. 3.3 mL; $P < 0.001$) or by CE-MRI (10.6 vs. 2.5 mL; $P = 0.001$). No significant differences were observed in patient age, sex, peritumoral edema, or meningiomatosis (each with $P > 0.05$). The detailed characteristics of extraosseous and transosseous meningiomas are shown in Table 1. A patient example is provided in Figure 1. Additional statistical analyses did not confirm statistically significant correlations between higher tracer uptake values and larger meningioma volumes (each with $P > 0.05$) and are provided in Supplemental Tables 1 and 2.

Diagnostic Performance of ^{68}Ga-DOTATATE PET/CT and CE-MRI for Detection of Osseous Involvement in Intracranial Meningiomas

The diagnostic accuracy for the two diagnostic tests was determined by defining the readers' interpretation of "consistent with" as positive. The overall sensitivity for osseous involvement of ^{68}Ga-DOTATATE PET/CT was significantly higher than that of CE-MRI (98.5% vs. 53.7%; $P < 0.001$). The overall specificity for osseous involvement of ^{68}Ga-DOTATATE PET/CT was high, although slightly lower than that of CE-MRI (86.7% vs. 93.3%; $P = 0.200$).

TABLE 4
PET/CT Measurements in Transosseous Meningiomas

Parameter	Overall (n = 67)	Parafalcine/ parasagittal (n = 10)	Convexity (n = 12)	Sphenoid wing (n = 42)	Cerebellopontine (n = 2)	Suprasellar/ parasellar (n = 1)
SUV_{max} total	14.2 (10–22)	10.8 (7–12)	15.6 (10–31)	14.8 (11–26)	7.3 (6–9)	12.6 (13–13)
SUV_{max} intraosseous	13.4 (10–22)	10.0 (7–11)	15.6 (10–31)	14.2 (11–26)	7.3 (6–9)	12.6 (13–13)
SUV_{mean} total	4.3 (3–6)	3.7 (3–4)	4.7 (3–7)	4.5 (4–6)	2.6 (3–3)	4.5 (4–4)
SUV_{mean} intraosseous	4.6 (3–7)	3.4 (3–4)	5.7 (3–8)	5.0 (4–8)	2.7 (3–3)	4.8 (5–5)
Volume total (mL)	12.8 (7–33)	6.4 (4–15)	13.3 (5–18)	17.7 (10–47)	5.6 (3–9)	9.9 (10–10)
Volume intraosseous (mL)	6.8 (3–15)	2.7 (1–5)	5.1 (2–11)	9.3 (6–21)	4.1 (2–7)	6.8 (7–7)

Data are median followed by interquartile range. SUV_{mean} in total meningioma compared with intraosseous part of meningioma showed statistically significant differences on Wilcoxon signed rank testing ($P < 0.001$).

The McNemar test showed significant differences in the diagnostic performance of the two methods ($P < 0.001$). The detailed diagnostic accuracy measures are presented in Table 2.

A receiver-operating-characteristic analysis for osseous involvement in the overall study population allows accounting for the 3-point scale of qualitative ^{68}Ga-DOTATATE PET/CT and CE-MRI assessment. Qualitative assessment produced a larger area under the curve using PET/CT than using CE-MRI (0.932 vs. 0.773). The detailed results are shown in Table 3. A graphic depiction of the receiver-operating-characteristic curves is provided in Supplemental Figure 2.

PET/CT Measurements in Transosseous Meningiomas

We compared the quantitative PET/CT measurements in the total tumor and in the segmented intraosseous tumor part to assess whether ^{68}Ga-DOTATATE PET/CT provides adequate signal within the bone. We stratified the analysis for different meningioma locations. The intraosseous SUV_{max} equaled the total SUV_{max} in almost every location. Overall, the intraosseous SUV_{mean} was significantly higher than the total SUV_{mean} (4.6 vs. 4.3; $P < 0.001$). The detailed results are provided in Table 4. Signal measurements in transosseous meningiomas with consistent imaging diagnoses of osseous involvement on ^{68}Ga-DOTATATE PET/CT and CE-MRI demonstrated significantly higher tumor-to-background signal for PET/CT than for CE-MRI for both the extraosseous part (13.4 vs. 3.7; $P < 0.001$) and the intraosseous part (7.5 vs. 1.9; $P < 0.001$). The results are shown in Supplemental Table 3.

Meningioma Volume Estimation Using ^{68}Ga-DOTATATE PET/CT and CE-MRI

Separate volumetric assessments of the meningioma using ^{68}Ga-DOTATATE PET/CT and CE-MRI yielded comparable results for extraosseous meningiomas (3.2 vs. 2.5 mL; $P = 0.132$) and the extraosseous part of transosseous meningiomas (6.6 vs. 6.7 mL; $P = 0.636$) based on the Wilcoxon signed rank test. In contrast, the intraosseous part of transosseous meningiomas was assessed as having significantly larger volumes by PET/CT (6.8 vs. 3.3 mL; $P < 0.001$). Consistently, analyses using Spearman correlation demonstrated lower correlation coefficients for the volume estimates of the intraosseous part of transosseous meningiomas ($r = 0.753$) than for the volume estimates of the extraosseous part ($r = 0.988$). The individual results are shown in a correlation scatterplot in Figure 2 and in a grouped volume plot in Supplemental Figure 3. Subgroup analyses for different meningioma locations returned similar relations in volume estimation; the results are presented in Figure 3. A representative patient example for the discrepancy in estimating the intraosseous meningioma volume is presented in Figure 4.

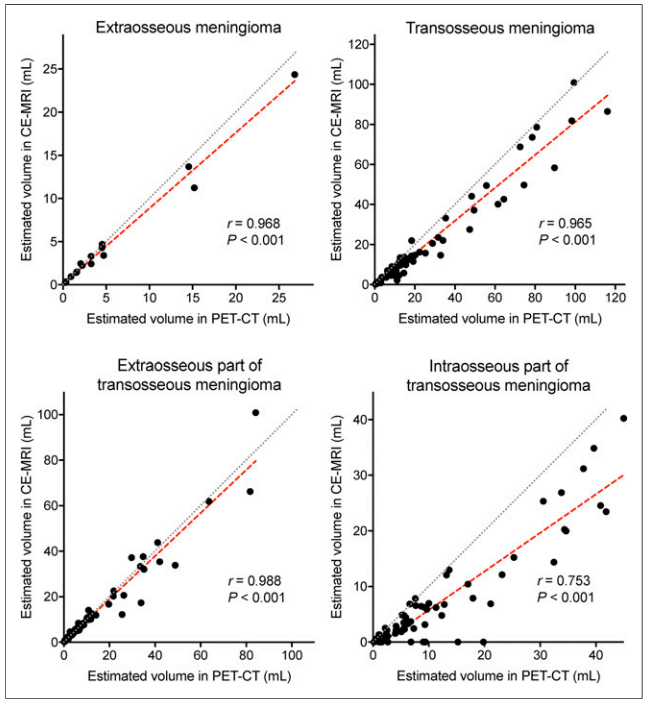

FIGURE 2. Comparison of estimated volumes in ^{68}Ga-DOTATATE PET/CT and CE-MRI. Correlation scatterplots depict estimated volumes using ^{68}Ga-DOTATATE PET/CT (x-axis) against estimated volumes using CE-MRI (y-axis). Spearman correlation coefficients (r) were calculated. Gray line represents perfect positive correlation. Red line is calculated using least-squares fit of data. Data are based on 82 meningioma patients with pathologic exclusion or inclusion of osseous involvement. In cases of imaging-based false-negative osseous involvement, intraosseous part was attributed no volume (0 mL). Wilcoxon signed rank test demonstrated significant differences between PET and CE-MRI for volume estimation of total and intraosseous part of transosseous meningiomas (each with $P < 0.001$).

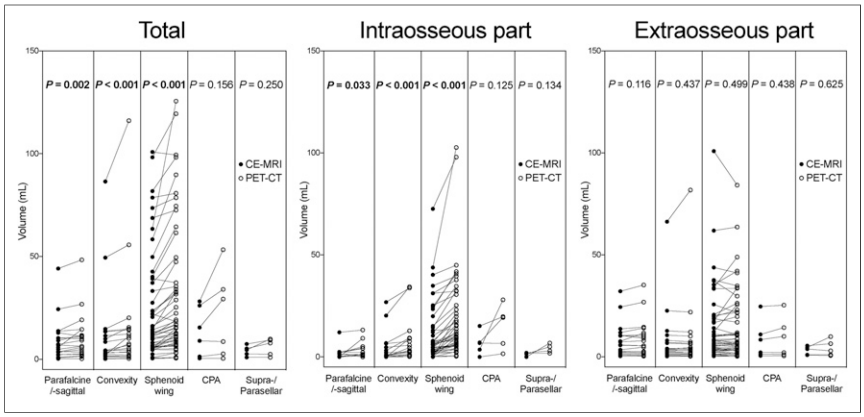

FIGURE 3. Comparison of estimated volumes stratified for meningioma location. Plots depict estimated volumes for total meningioma, intraosseous part, and extraosseous part using ^{68}Ga-DOTATATE PET/CT (open circles) and CE-MRI (solid circles). Data are based on 105 meningioma patients, among whom 90 had imaging-based diagnosis of transosseous extension. Statistical comparison was performed using Wilcoxon signed rank test. Bold *P* values indicate statistical significance. CPA = cerebellopontine angle.

DISCUSSION

The recently published European Association of Neuro-Oncology guidelines for the diagnosis and treatment of meningiomas by Goldbrunner et al. (*2*) reinforced the role of CE-MRI as the primary imaging modality of choice. However, the authors also underlined the considerable diagnostic challenges in the delineation of meningiomas, particularly in complex locations such as the skull base. The limited sensitivity of CE-MRI for the diagnosis of osseous involvement in our study is in line with a previous study comparing ^{18}F-fluoride PET/CT with CE-MRI by Tateishi et al. (*21*). ^{68}Ga-DOTATATE PET/CT provided an improved detection of osseous involvement similar to that of ^{18}F-fluoride PET/CT based on the comparison of receiver-operating-characteristic analyses. In ^{18}F-fluoride PET/CT, intraosseous meningioma extension is indirectly estimated by osseous ^{18}F-fluoride tracer uptake, reflecting active bone formation and osseous turnover (*22*). In contrast, ^{68}Ga-DOTATATE directly binds to meningioma tissue characterized by somatostatin-receptor overexpression.

The higher ^{68}Ga-DOTATATE tracer uptake of transosseous meningiomas is in line with a previous report by Sommerauer et al. (*12*), which originally investigated the prognostic information of tracer uptake for growth prediction. Investigating a larger number of patients with transosseous meningiomas, we can confirm this observation. Notably, we did not detect a significant interrelation between meningioma volume and ^{68}Ga-DOTATATE uptake values. Both the extraosseous and the intraosseous parts of transosseous meningiomas demonstrated strong tracer uptake. The slightly higher SUV_{mean} of the intraosseous part than of the total meningioma is likely explained by the adaptation of the VOI, which may neglect areas of the tumor rim with lower tracer uptake. The difference in tracer uptake between extraosseous and transosseous meningiomas is interesting regarding its impact on growth prediction (*12*), as attempts to draw prognostic information from MRI parameters failed (*25*). As outlined by the recent European Association of Neuro-Oncology guidelines (*2*), evidence regarding surveillance and follow-up is scarce and recommendations were thus based on expert consensus opinion. In this respect, ^{68}Ga-DOTATATE PET/CT has the potential to identify additional risk factors for tumor growth such as osseous involvement (*13*) or tracer uptake to guide the timing of follow-up imaging and improve patient surveillance.

Volumetric assessment of meningiomas using conventional imaging such as CE-MRI is cumbersome and often poorly approximated in daily clinical routine by the ABC/2 formula (*26*), thus introducing a considerable risk for misdiagnosis of tumor progression. Thereby, important prognostic information is neglected, as computer-aided volumetric analyses of meningiomas have proven to be more accurate in the assessment of tumor growth than the above-mentioned approximated volumes (*27*). In this light, ^{68}Ga-DOTATATE PET/CT may facilitate automated volume measurements based on the PET tracer uptake, which provides improved tumor-to-background signal. A prior prospective study by Rachinger et al. (*24*) established an SUV_{max} cutoff of 2.3 for discrimination between meningioma and tumor-free tissue by spatially precise neuronavigated tissue-sampling during surgical resection. We applied this cutoff for the volume estimation by PET/CT and found good agreement with CE-MRI for extraosseous meningiomas and the extraosseous part of transosseous meningiomas. Given these features, ^{68}Ga-DOTATATE PET/CT could make volume measurements and successive comparisons easily accessible in clinical routine and thereby improve therapy guidance. The intraosseous in contrast to the extraosseous part of transosseous meningiomas, however, showed considerable differences in volume estimation, as

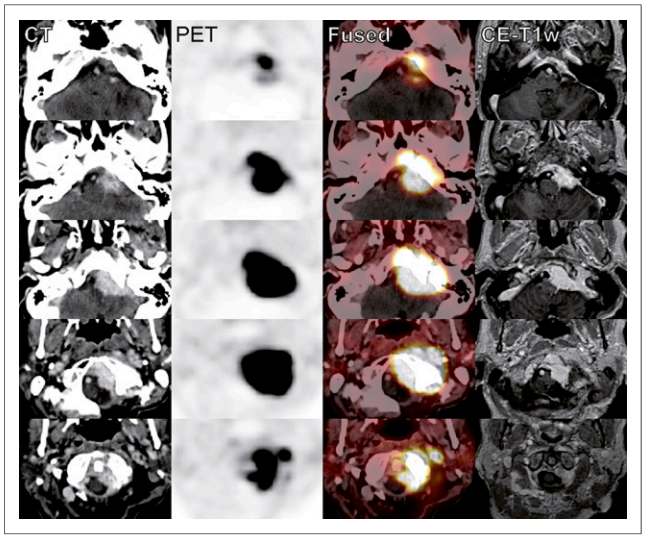

FIGURE 4. Example of estimated intraosseous volume discrepancy between ^{68}Ga-DOTATATE PET/CT and CE-MRI in patient with skull base meningioma. A 75-y-old woman was followed up with ^{68}Ga-DOTATATE PET/CT and CE-MRI after partial resection of transosseous transitional meningioma (World Health Organization grade I) in left cerebellopontine angle. Because of worsening and radiating pain in occipital region and hypoglossal nerve palsy, she was evaluated for stereotactic radiosurgery. Estimated volumes of transosseous extension were significantly larger on ^{68}Ga-DOTATATE PET/CT than on CE-MRI (28.0 vs. 7.5 mL), whereas volumes of extraosseous part agreed well (25.3 vs. 22.6 mL). w = weighted.

significantly larger intraosseous meningioma volumes were obtained using ^{68}Ga-DOTATATE PET/CT than using CE-MRI. These differences might be explained by the considerably higher tumor-to-background signal that is provided by ^{68}Ga-DOTATATE PET/CT. Visual comparison of the intraosseous PET and CE-MRI VOI shapes frequently revealed a very asymmetric distribution of the larger PET VOI around the CE-MRI VOI, exposing intraosseous meningioma extension undetected by CE-MRI. Because of this asymmetry between the PET and CE-MRI VOIs, a systematic overestimation of intraosseous meningioma extension by PET caused by spillover remains unlikely. On the basis of the differences in intraosseous as opposed to extraosseous volume estimation, we hypothesize, but cannot prove, that CE-MRI may underestimate the transosseous extension of intracranial meningiomas.

^{68}Ga-DOTATATE PET adds important diagnostic molecular information to the primarily anatomic imaging modalities CT and MRI. Analogous to integrated PET/CT, hybrid PET/MRI scanners enable simultaneous acquisition of PET and MR images combining molecular PET information with high-resolution MR images yielding superior soft-tissue contrast. In addition, integrated acquisition of PET and MRI data provides optimized temporal and spatial data coregistration superior to software-based image fusion of separately acquired PET and MR images (*28*). In a comparison of ^{68}Ga-DOTATOC PET/CT and PET/MRI for meningioma imaging, Afshar-Oromieh et al. demonstrated the feasibility of ^{68}Ga-DOTATOC PET/MRI for the detection of intracranial meningiomas in a cohort of 15 patients (*29*). The authors reported that the acquired PET/MR images were free of artifacts and concluded that ^{68}Ga-DOTATOC PET/MRI represents an ideal combination of high sensitivity and specificity with the best morphologic visualization. However, with regard to the comparison to ^{68}Ga-DOTATOC PET/CT, the authors stated that no superiority of PET/MRI for treatment planning could be shown in this cohort and that larger studies are needed to compare the two techniques. In favor of PET/CT, important diagnostic CT information includes high-resolution bone imaging. Dedicated CT protocols aid in the localization of intraosseous meningioma manifestations and enable precise preoperative planning, particularly in difficult locations such as the skull base. In the case of calcified meningiomas, CT supports the assessment of gross tumor volume in radiation therapy planning, whereas calcifications cause extinction artifacts on MRI (5). Therefore, all 3 modalities—PET, MRI, and CT—contribute important information to diagnosis and treatment planning in meningioma. With ^{68}Ga-DOTATATE PET as the most sensitive modality for the assessment of meningioma manifestations, the selection of either hybrid imaging modality, PET/CT or PET/MRI, is feasible. The third modality can be acquired separately, depending on clinical preference and availability.

There are limitations to our study that need to be considered when interpreting the data. First, pathologic confirmation of inclusion or exclusion of osseous involvement as the prerequisite for a study on diagnostic accuracy represents a selection bias toward symptomatic meningioma patient subgroups in which surgical resection was indicated. Second, the consecutive cohort of patients undergoing ^{68}Ga-DOTATATE PET/CT examinations may cause a selection bias to patients with meningiomas in complex anatomic locations or with inconclusive MRI examinations. Third, the estimation of meningioma volumes could not be compared with a pathologic standard of reference because surgical resections were sometimes intended as partial resections or the resection material is too fragmented for ex vivo volume analysis. Therefore, no evidence on the pathologic meningioma volumes can be drawn. Yet, to our knowledge, this study represents the largest cohort of patients evaluated for osseous involvement by ^{68}Ga-DOTATATE PET/CT and CE-MRI with pathologic confirmation as the standard of reference.

CONCLUSION

The present study evaluated the diagnostic performance of ^{68}Ga-DOTATATE PET/CT and CE-MRI for the detection of osseous involvement by intracranial meningiomas, with pathology-proven bone infiltration as the standard of reference. ^{68}Ga-DOTATATE PET/CT provided a higher sensitivity than CE-MRI while maintaining high specificity. Quantitative PET/CT analysis confirmed adequate tracer distribution in intraosseous meningioma parts and yielded significantly higher tumor-to-background signals than CE-MRI. Volumetric analysis using ^{68}Ga-DOTATATE PET/CT returned significantly larger volume estimates for the intraosseous extension of transosseous meningiomas than CE-MRI, whereas the estimated volumes for extraosseous meningioma parts did not differ significantly between the two methods. ^{68}Ga-DOTATATE PET/CT provides added diagnostic value in the assessment of transosseous meningiomas compared with CE-MRI.

DISCLOSURE

No potential conflict of interest relevant to this article was reported.

REFERENCES

1. Wiemels J, Wrensch M, Claus EB. Epidemiology and etiology of meningioma. *J Neurooncol.* 2010;99:307–314.
2. Goldbrunner R, Minniti G, Preusser M, et al. EANO guidelines for the diagnosis and treatment of meningiomas. *Lancet Oncol.* 2016;17:e383–e391.
3. Di Chiro G, Hatazawa J, Katz DA, Rizzoli HV, De Michele DJ. Glucose utilization by intracranial meningiomas as an index of tumor aggressivity and probability of recurrence: a PET study. *Radiology.* 1987;164:521–526.
4. Lippitz B, Cremerius U, Mayfrank L, et al. PET-study of intracranial meningiomas: correlation with histopathology, cellularity and proliferation rate. *Acta Neurochir Suppl.* 1996;65:108–111.
5. Suchorska B, Tonn JC, Jansen NL. PET imaging for brain tumor diagnostics. *Curr Opin Neurol.* 2014;27:683–688.
6. Henze M, Dimitrakopoulou-Strauss A, Milker-Zabel S, et al. Characterization of ^{68}Ga-DOTA-D-Phe1-Tyr3-octreotide kinetics in patients with meningiomas. *J Nucl Med.* 2005;46:763–769.
7. Henze M, Schuhmacher J, Hipp P, et al. PET imaging of somatostatin receptors using [^{68}GA]DOTA-D-Phe^{1}-Tyr^{3}-octreotide: first results in patients with meningiomas. *J Nucl Med.* 2001;42:1053–1056.
8. Afshar-Oromieh A, Giesel FL, Linhart HG, et al. Detection of cranial meningiomas: comparison of ^{68}Ga-DOTATOC PET/CT and contrast-enhanced MRI. *Eur J Nucl Med Mol Imaging.* 2012;39:1409–1415.
9. Nyuyki F, Plotkin M, Graf R, et al. Potential impact of ^{68}Ga-DOTATOC PET/CT on stereotactic radiotherapy planning of meningiomas. *Eur J Nucl Med Mol Imaging.* 2010;37:310–318.
10. Seystahl K, Stoecklein V, Schuller U, et al. Somatostatin receptor-targeted radionuclide therapy for progressive meningioma: benefit linked to ^{68}Ga-DOTATATE/-TOC uptake. *Neuro-oncol.* 2016;18:1538–1547.
11. Collamati F, Pepe A, Bellini F, et al. Toward radioguided surgery with β^- decays: uptake of a somatostatin analogue, DOTATOC, in meningioma and high-grade glioma. *J Nucl Med.* 2015;56:3–8.
12. Sommerauer M, Burkhardt JK, Frontzek K, et al. ^{68}Gallium-DOTATATE PET in meningioma: a reliable predictor of tumor growth rate? *Neuro Oncol.* 2016;18:1021–1027.
13. Kallio M, Sankila R, Hakulinen T, Jaaskelainen J. Factors affecting operative and excess long-term mortality in 935 patients with intracranial meningioma. *Neurosurgery.* 1992;31:2–12.

14. Jääskeläinen J. Seemingly complete removal of histologically benign intracranial meningioma: late recurrence rate and factors predicting recurrence in 657 patients—a multivariate analysis. *Surg Neurol.* 1986;26:461–469.
15. Sankila R, Kallio M, Jääskeläinen J, Hakulinen T. Long-term survival of 1986 patients with intracranial meningioma diagnosed from 1953 to 1984 in Finland: comparison of the observed and expected survival rates in a population-based series. *Cancer.* 1992;70:1568–1576.
16. Ildan F, Erman T, Gocer AI, et al. Predicting the probability of meningioma recurrence in the preoperative and early postoperative period: a multivariate analysis in the midterm follow-up. *Skull Base.* 2007;17:157–171.
17. Terstegge K, Schorner W, Henkes H, Heye N, Hosten N, Lanksch WR. Hyperostosis in meningiomas: MR findings in patients with recurrent meningioma of the sphenoid wings. *AJNR Am J Neuroradiol.* 1994;15:555–560.
18. Arana E, Diaz C, Latorre FF, et al. Primary intraosseous meningiomas. *Acta Radiol.* 1996;37:937–942.
19. Hamilton BE, Salzman KL, Patel N, et al. Imaging and clinical characteristics of temporal bone meningioma. *AJNR Am J Neuroradiol.* 2006;27:2204–2209.
20. Bikmaz K, Mrak R, Al-Mefty O. Management of bone-invasive, hyperostotic sphenoid wing meningiomas. *J Neurosurg.* 2007;107:905–912.
21. Tateishi U, Tateishi K, Hino-Shishikura A, Torii I, Inoue T, Kawahara N. Multimodal approach to detect osseous involvement in meningioma: additional value of ^{18}F-fluoride PET/CT for conventional imaging. *Radiology.* 2014;273:521–528.
22. Tateishi U, Tateishi K, Shizukuishi K, et al. ^{18}F-fluoride PET/CT allows detection of hyperostosis and osseous involvement in meningioma: initial experience. *Clin Nucl Med.* 2013;38:e125–e131.
23. Louis DN, Ohgaki H, Wiestler OD, et al. The 2007 WHO classification of tumours of the central nervous system. *Acta Neuropathol (Berl).* 2007;114:97–109.
24. Rachinger W, Stoecklein VM, Terpolilli NA, et al. Increased ^{68}Ga-DOTATATE uptake in PET imaging discriminates meningioma and tumor-free tissue. *J Nucl Med.* 2015;56:347–353.
25. Schob S, Frydrychowicz C, Gawlitza M, et al. Signal intensities in preoperative MRI do not reflect proliferative activity in meningioma. *Transl Oncol.* 2016;9:274–279.
26. Ishi Y, Terasaka S, Yamaguchi S, et al. Reliability of the size evaluation method for meningiomas: maximum diameter, ABC/2 formula, and planimetry method. *World Neurosurg.* 2016;94:80–88.
27. Chang V, Narang J, Schultz L, et al. Computer-aided volumetric analysis as a sensitive tool for the management of incidental meningiomas. *Acta Neurochir (Wien).* 2012;154:589–597.
28. Boss A, Bisdas S, Kolb A, et al. Hybrid PET/MRI of intracranial masses: initial experiences and comparison to PET/CT. *J Nucl Med.* 2010;51:1198–1205.
29. Afshar-Oromieh A, Wolf MB, Kratochwil C, et al. Comparison of ^{68}Ga-DOTATOC-PET/CT and PET/MRI hybrid systems in patients with cranial meningioma: initial results. *Neuro-oncol.* 2015;17:312–319.